ARTICLE

doi:10.1038/nature11315

RPN-6 determines *C. elegans* longevity under proteotoxic stress conditions

David Vilchez[1], Ianessa Morantte[1], Zheng Liu[1], Peter M. Douglas[1], Carsten Merkwirth[1], Ana P. C. Rodrigues[2]†, Gerard Manning[2]† & Andrew Dillin[1]

Organisms that protect their germ-cell lineages from damage often do so at considerable cost: limited metabolic resources become partitioned away from maintenance of the soma, leaving the ageing somatic tissues to navigate survival amid an environment containing damaged and poorly functioning proteins. Historically, experimental paradigms that limit reproductive investment result in lifespan extension. We proposed that germline-deficient animals might exhibit heightened protection from proteotoxic stressors in somatic tissues. We find that the forced re-investment of resources from the germ line to the soma in *Caenorhabditis elegans* results in elevated somatic proteasome activity, clearance of damaged proteins and increased longevity. This activity is associated with increased expression of *rpn-6*, a subunit of the 19S proteasome, by the FOXO transcription factor DAF-16. Ectopic expression of *rpn-6* is sufficient to confer proteotoxic stress resistance and extend lifespan, indicating that *rpn-6* is a candidate to correct deficiencies in age-related protein homeostasis disorders.

In nature, food sources are largely unpredictable and insufficient. The constant pressures that limited energetic resources place on an organism have long been theorized to cause a significant life-history trade-off: the absolute need for repairing and preventing damage to the germ line, and for ensuring elimination of damage in progeny, necessarily dominates resource allocation strategies, whereas conversely little or no evolutionary pressure will be placed on the maintenance of the soma[1]. Thus, ageing, post-reproductive organisms that escape predation witness the gradual deterioration of their own somatic tissues. In support of such theories, modulations of reproduction that eliminate germ cells provide effective mechanisms for extending lifespan[2,3], phenotypes that may be caused by heightened resource availability within the post-mitotic soma. Likewise, it has been proposed that animals undergoing dietary restriction adopt a strategy in which resources are re-allocated towards somatic maintenance, extending lifespan and prolonging reproduction until conditions for survival become more favourable[4].

When proliferating germline cells of *C. elegans* are removed, worms live up to 60% longer than normal and seem to be resistant to a variety of environmental stressors[5–7]. Whereas germline ablation affords an obvious protection, the downstream effectors of such protection remain ambiguous. The re-allocation of resources to the soma seems to be directed through a specific, genetically defined stress-responsive pathway. Germline removal extends lifespan by triggering an active signalling network, involving the nuclear localization and activation of DAF-16, a forkhead transcription factor (FOXO)[8] and the major downstream effector of the DAF-2–insulin–insulin-like growth factor (IGF) signalling (IIS) pathway. However, although worms with an ablated germ line exhibit a *daf-16*-dependent extension in lifespan, longevity caused by germline ablation functions in a synergistic manner with mutations in the IIS receptor, *daf-2* (ref. 6). Additionally, in germline-ablated animals, but not *daf-2* mutant worms, *kri-1*, *daf-9* and the nuclear hormone receptor *daf-12* are also required for the constitutive nuclear localization of DAF-16 (refs 9, 10).

Notably, post-mitotic somatic cells are particularly susceptible to age-onset protein aggregation diseases. As the somatic cell ages, the accumulation of damaged proteins represents a particular challenge to the ageing cell, especially as they aggregate in inclusions and aggresomes capable of overwhelming the cellular machinery required for their degradation[11,12]. These effects are probably compounded by age-related dysregulation of chaperones, a downregulation of degradation machinery itself, and a continually accelerating loss in general cellular homeostasis. As such, a rapid decline in the capacity of the cell to protect its proteome has been highly correlated with multiple age-related disorders[13]. This conversely indicates that long-lived somatic cells, such as those found in a germline-ablated animal, might exhibit a heightened capacity for clearing damaged proteins, and that this proteostatic capacity might contribute to the increased longevity in these mutants.

Increased proteasome activity in *glp-1(e2141)* worms

We hypothesized that a key aspect of the proteostasis network, the ubiquitin proteasome system (UPS), might be altered in the soma of germline-ablated animals. To test this hypothesis, we first examined the activity of the 26S/30S proteasome in several long-lived mutants using a fluorogenic peptide substrate specific for the chymotrypsin-like activity of the proteasome (Supplementary Fig. 1). We found that *glp-1(e2141)* mutant worms, which lack their germ line, displayed a marked increase (over sixfold) in the chymotrypsin-like proteasome activity (Fig. 1a and Supplementary Figs 1 and 2a–c). The proteasome inhibitors MG-132, lactacystin and PI-I blocked activity from extracts in both the *glp-1* mutant and the control strain (Supplementary Fig. 3), indicating that the increased peptidase activity in *glp-1(e2141)* worms was due to the proteasome. The caspase-like and trypsin-like activities were also increased in *glp-1* mutant worms (Fig. 1b, c). Additionally, we found that a *C. elegans* genetic model of dietary restriction[14] also induced proteasome activity, although to a lesser extent than the *glp-1(e2141)* mutation (Supplementary Fig. 1). In contrast, neither reduced IIS signalling by mutation of *daf-2* nor reduced mitochondrial

[1]Howard Hughes Medical Institute, Glenn Center for Aging Research, Molecular and Cell Biology Laboratory, The Salk Institute for Biological Studies, 10010 North Torrey Pines Road, La Jolla, California 92037, USA. [2]Razavi Newman Center for Bioinformatics, The Salk Institute for Biological Studies, 10010 North Torrey Pines Road, La Jolla, California 92037, USA. †Present addresses: Department of Computational Medicine and Bioinformatics, University of Michigan, 100 Washtenaw Avenue, Ann Arbor, Michigan 48109-2218, USA (A.P.C.R.); Bioinformatics and Computational Biology, Genentech, 1 DNA Way, South San Francisco, California 94080, USA (G.M.).

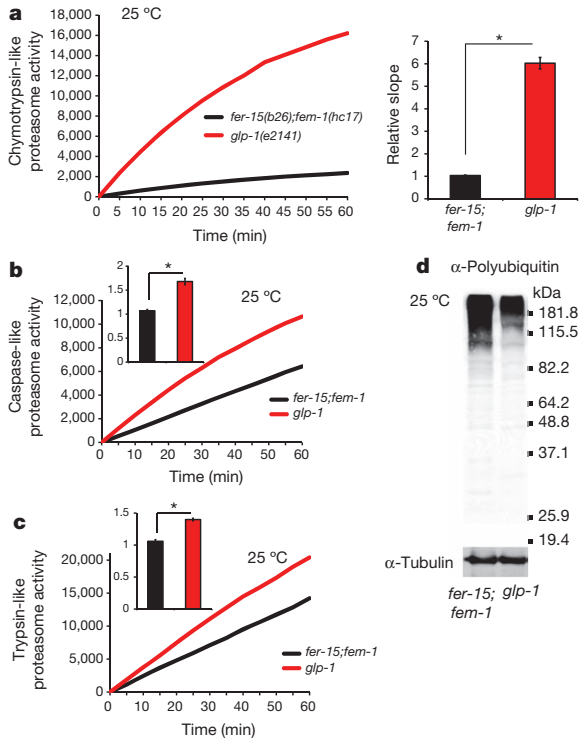

Figure 1 | Germline-lacking nematodes have increased proteasome activity. **a**, Chymotrypsin-like activity of the proteasome monitored by Z-Gly-Gly-Leu-AMC digestion in day 7 adult worm extract containing equal amounts of total protein. Proteasome activity (relative slope to control strain *fer-15(b26);fem-1(hc17)*) is shown, with error bars indicating mean ± s.e.m. ($n = 50$, $^*P = 1.83 \times 10^{-17}$). **b**, Caspase-like (Z-Leu-Leu-Glu-AMC) proteasome activity (relative slope) is shown, with error bars representing mean ± s.e.m. ($n = 8$, $^*P < 0.00001$). **c**, Trypsin-like (Ac-Arg-Leu-Arg-AMC) proteasome activity (relative slope) is shown, with error bars showing mean ± s.e.m. ($n = 7$, $^*P < 0.00001$). **d**, Representative polyubiquitinated protein immunoblot. α-Tubulin is used as the loading control.

electron transport chain activity[15] upregulated proteasome activity (Supplementary Fig. 1). Consistent with increased proteasome activity in *glp-1(e2141)* worms, we observed decreased levels of polyubiquitinated proteins in these worms (Fig. 1d). To examine further UPS activity in living animals, we used a photoconvertible fluorescent UPS reporter system for live imaging and quantification of protein degradation in *C. elegans*[16]. This proteasome reporter consists of the photoconvertible fluorescent protein Dendra2 targeted for proteasomal degradation by fusion to a mutant form of ubiquitin (UbG76V) that cannot be cleaved by ubiquitin hydrolases. Dendra2 can be irreversibly photoconverted from a green to a red fluorescent state, providing quantification of UPS activity independently of protein synthesis. We found that this reporter is degraded more rapidly in *glp-1* mutant worms compared to control strains, whereas Dendra2 lacking the UbG76V signal remained stable (Supplementary Fig. 4).

glp-1(e2141) worms differ from other types of reproductive mutants in that their entire germ line is missing. Notably, *glp-1* mutants exhibit a significantly increased lifespan in comparison to worms that are also sterile but which still contain a proliferating germ line (Supplementary Fig. 5). We observed that the increased proteasome activity of *glp-1* mutants was not due to a benefit of sterility per se, because the normal-lived, sterile control *fer-15(b26);fem-1(hc17)* animals have similar proteasome activity as wild-type animals (Supplementary Figs 2a and 6). Furthermore, treatment with 5-fluoro-2′deoxyuridine (FUdR), a drug used to block progeny production in worms[17], did not affect proteasome activity (Supplementary Fig. 6). The *glp-1(e2141)* allele is temperature-sensitive for reproduction and longevity[18]; these worms are only long-lived when they are shifted to restrictive temperature (25 °C) either during development or in early adulthood[5]. Accordingly, proteasome activity is not increased in *glp-1(e2141)* worms grown continuously at the permissive temperature (Supplementary Fig. 7). However, resembling the longevity phenotype[5], *glp-1(e2141)* worms maintained high proteasome activity when down-shifted to a permissive temperature after germline removal (Supplementary Fig. 8). These results indicate that different forms of sterility do not have similar effects on proteasome activity, but are specific to loss of the germ line.

DAF-16 regulates proteasome activity

Because DAF-16, the worm FOXO transcription factor, is essential for the increased longevity of *glp-1* mutant worms[5], we tested whether *daf-16* was also required for the increased proteasome activity found in *glp-1(e2141)* animals. Proteasome activity of *glp-1* mutant animals was suppressed to wild-type levels in *daf-16;glp-1* double mutant animals (Fig. 2a–c). *daf-16* is required during reproductive adulthood to modulate the ageing process in worms[19]. Accordingly, *daf-16* RNA interference (RNAi) treatment of *glp-1(e2141)* animals during adulthood decreased proteasome activity (Fig. 2d). In contrast, *daf-16* RNAi did not affect proteasome activity in control strains (Fig. 2d and Supplementary Fig. 9), where DAF-16 is located in the cytosol and is inactive. Loss of *daf-16* suppressed longevity and proteasome activity, but not the reproductive phenotype of *glp-1(e2141)* worms, providing further evidence that increased proteasomal activity could not be separated from the increased longevity mediated by DAF-16 in *glp-1* mutants. We examined whether other genes required to promote DAF-16/FOXO nuclear localization in the germline longevity pathway (that is, *daf-12*, *daf-9* and *kri-1*) were also necessary for increased proteasome activity. Accordingly, reduction of any one of these genes in *glp-1(e2141)* worms resulted in decreased proteasome activity, although not to the extent of *daf-16* reduction (Fig. 2e). Furthermore, reduction of *daf-12*, *daf-9* or *kri-1* did not further decrease proteasome activity of the *daf-16;glp-1* double mutant animals or the control strain (Supplementary Fig. 10a, b). In addition to *daf-16*, *glp-1*-mediated longevity requires two additional transcription factors: *hsf-1* (ref. 20) and *skn-1* (Supplementary Fig. 11). *hsf-1* is required for the regulation of adult lifespan, heat-shock and proteotoxic stress[21,22]; *skn-1* is the worm orthologue of *nrf-2* and has a central role in oxidative stress responses in worms, flies and mice[23,24]. In contrast to *daf-16*, *daf-12*, *daf-9* and *kri-1*, we observed that neither *hsf-1* nor *skn-1* was required for the increased proteasome activity in *glp-1(e2141)* worms (Fig. 2f, g). To uncover a possible redundancy of either *hsf-1* or *skn-1* with *daf-16*, we knocked down these factors in the *daf-16;glp-1* double mutant animals. However, in the context of *daf-16* loss, neither *hsf-1* nor *skn-1* further affected proteasome activity in *glp-1(e2141)* worms (Supplementary Fig. 12). The nuclear hormone receptor *nhr-80* links fatty acid desaturation to lifespan extension through germline ablation in a *daf-16*-independent manner[25]. Consistent with a requirement for *daf-16* in proteasome activity, *nhr-80* was not required for increased proteasome activity in *glp-1* mutant worms (Supplementary Fig. 13). Taken together, alterations that specifically affect DAF-16 activity, but not HSF-1, SKN-1 or NHR-80, alter proteasome activity in *glp-1* mutants, indicating that a major output for DAF-16-mediated longevity in this mutant is to increase proteasome activity.

DAF-16 regulates *rpn-6.1* levels

The 26S/30S proteasome consists of a 20S core structure that contains the proteolytic active sites and 19S cap structures that impart regulation on the activity of the holo-complex (26S, single capped, and 30S, double capped)[26]. Although 20S particles can exist in a free form, 20S particles in their most physiological form are inactive, unable to degrade denatured proteins or cleave peptides[27]. The 19S regulatory subunit is responsible for stimulating the 20S proteasome to degrade proteins, as ATPases of the regulatory particle open the 20S core, allowing substrates access to proteolytic active sites[28]. Analysis of

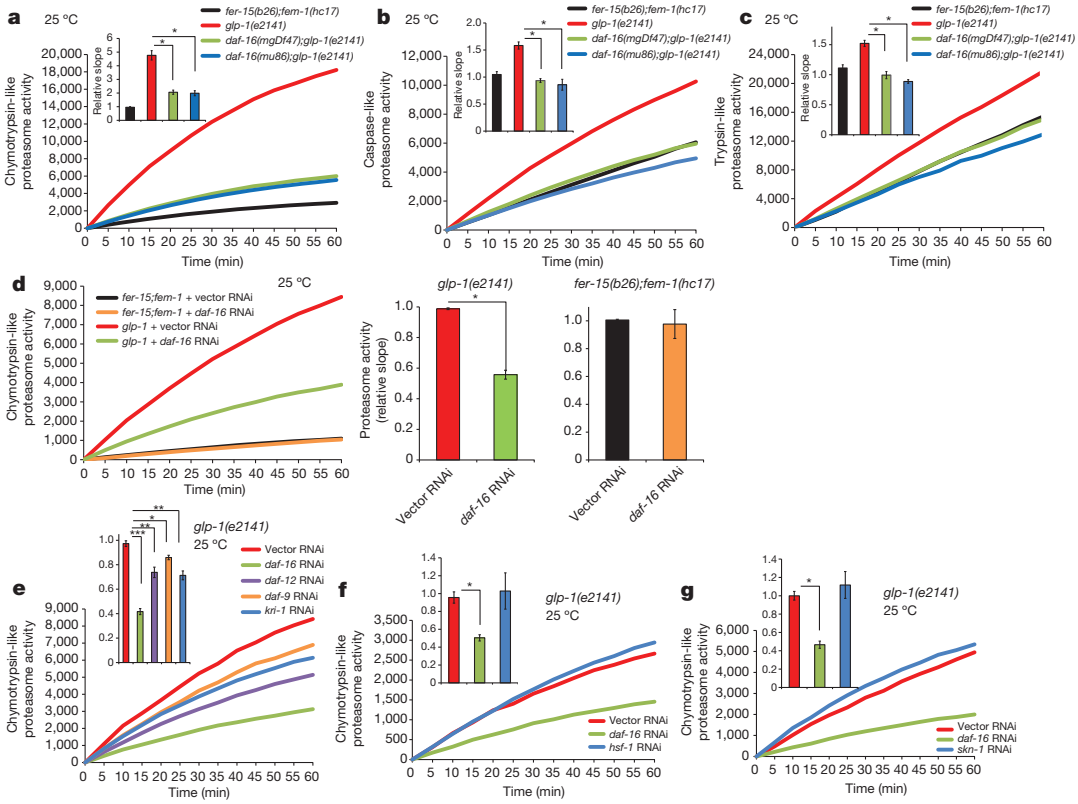

Figure 2 | DAF-16 is required for proteasome activity in *glp-1(e2141)* mutant nematodes. **a**, Chymotrypsin-like proteasome activity (relative slope to *fer-15(b26);fem-1(hc17)*) is shown. Error bars indicate mean ± s.e.m. ($n = 11$, $^*P < 0.00005$). **b**, Caspase-like proteasome activity (relative slope to *fer-15(b26);fem-1(hc17)*) is shown. Error bars indicate mean ± s.e.m. ($n = 6$, $^*P < 0.0001$). **c**, Trypsin-like proteasome activity (relative slope to *fer-15(b26);fem-1(hc17)*) is shown. Error bars represent mean ± s.e.m. ($n = 6$, $^*P < 0.005$). **d**, *glp-1(e2141)* worms fed *daf-16* RNAi bacteria show decreased chymotrypsin-like proteasome activity ($P = 8.5 \times 10^{-8}$ *glp-1* mutant fed vector RNAi bacteria versus *glp-1* mutant fed *daf-16* RNAi bacteria; $n = 16$). *daf-16* RNAi knock down does not affect proteasome activity in *fer-15;fem-1* worms ($P = 0.79$ *fer-15;fem-1* fed vector RNAi bacteria versus *fer-15;fem-1* fed *daf-16* RNAi bacteria; $n = 9$). **e**, Chymotrypsin-like proteasome activity in *glp-1(e2141)* worms fed *daf-16*, *daf-12*, *daf-9* or *kri-1* RNAi bacteria ($n = 4$; vector RNAi versus *daf-16* RNAi ($P = 4.17 \times 10^{-5}$); vector RNAi versus *daf-12* RNAi ($P < 0.01$); vector RNAi versus *daf-9* RNAi ($P < 0.05$); vector RNAi versus *kri-1* RNAi ($P < 0.01$)). **f**, Chymotrypsin-like proteasome activity (relative slope to *glp-1* mutant fed vector RNAi bacteria) is shown. Error bars indicate mean ± s.e.m. ($n = 8$; vector RNAi versus *daf-16* RNAi ($P < 0.0001$); vector RNAi versus *hsf-1* RNAi ($P = 0.74$)). **g**, *skn-1* RNAi does not affect chymotrypsin-like proteasome activity of *glp-1(e2141)* worms (vector RNAi versus *daf-16* RNAi ($P < 0.00001$); vector RNAi versus *hsf-1* RNAi ($P = 0.46$)). Chymotrypsin-like proteasome activity (relative slope to *glp-1* mutant fed vector RNAi bacteria) is shown. Error bars indicate the mean ± s.e.m. ($n = 9$; vector RNAi versus *daf-16* RNAi ($P < 0.00001$); vector RNAi versus *hsf-1* RNAi ($P = 0.46$)). All activities measured at day 5 of adulthood. All RNAi treatment was initiated at day 1 of adulthood. All statistical comparisons were made by Student's *t*-test for unpaired samples.

the messenger RNA levels of the 20S proteasome subunits revealed that α-subunits were not increased in *glp-1* mutants whereas only one of the β-subunits, *pbs-5*, was moderately increased (Supplementary Fig. 14 and Supplementary Table 1). PBS-5 is the β-type subunit that contains the chymotrypsin-like proteolytic active site[26]. With regard to the 19S proteasome subunits, we did not detect an increase of the ATPase subunits (Fig. 3a and Supplementary Table 1). Notably, only one of the non-ATPase subunits showed increased mRNA levels in *glp-1* mutant animals: *rpn-6.1*, an essential subunit for the activity of the 26S/30S proteasome that stabilizes the otherwise weak interaction between the 20S core and the 19S cap[29,30] (Fig. 3a, b and Supplementary Table 1). mRNA levels of the closely related *rpn-6.2* were not increased in *glp-1* mutants (Fig. 3a and Supplementary Table 1). *rpn-6.1* had a threefold increase in its expression in *glp-1* mutants and was by far the most increased of all subunits. Accordingly, knock down of *rpn-6.1* markedly decreased proteasome activity in *glp-1(e2141)* animals (Fig. 3c) similar to loss of *daf-16*. In contrast, loss of other non-ATPase subunits did not affect proteasome activity of *glp-1* mutants (Supplementary Fig. 15). Knock down of *rpn-6.1* induced an upregulation in the expression of the rest of the 26S proteasome subunits, probably to compensate for the reduction in proteasome activity induced by decreased levels of this critical subunit (Supplementary Table 2). Moreover, overexpression of *rpn-6.1* in wild-type animals was sufficient to increase proteasome activity (Fig. 3d). The increase in *rpn-6.1* mRNA levels did not alter the expression of other 26S proteasome subunits (Supplementary Table 3). Taken together, RPN-6.1 seems to be a key component required for activation of the proteasome machinery of the germline-lacking nematodes.

We found that DAF-16 is necessary for the increased expression of *rpn-6.1* by analysing its mRNA levels in both *daf-16;glp-1* double mutants and *daf-16* RNAi-treated animals (Fig. 3e, Supplementary Figs 16 and 17 and Supplementary Table 4). Notably, mRNA levels of other proteasome subunits, including *pbs-5*, were not decreased by loss of *daf-16* in *glp-1* mutant worms (Supplementary Fig. 17). *daf-16* RNAi did not change *rpn-6.1* expression in control worms (Supplementary Fig. 16). Therefore, these results display a correlation between *daf-16* activity, *rpn-6.1* levels and proteasome activity. Consistent with DAF-16 regulating the expression of *rpn-6.1*, we identified a potential DAF-16 binding site[31] within the first intron of *rpn-6.1* (Supplementary Fig. 18). This site is supported by a DAF-16 binding region defined by the modENCODE project[32], indicating that *rpn-6.1* is likely to be a direct DAF-16 target. To explore further *rpn-6.1* transcriptional regulation, we generated a transcriptional reporter construct. We found that *rpn-6.1* was expressed in the pharynx and posterior intestine in control worms. Notably, *rpn-6.1* expression increased markedly in the pharynx and throughout the intestine of *glp-1* mutants. In

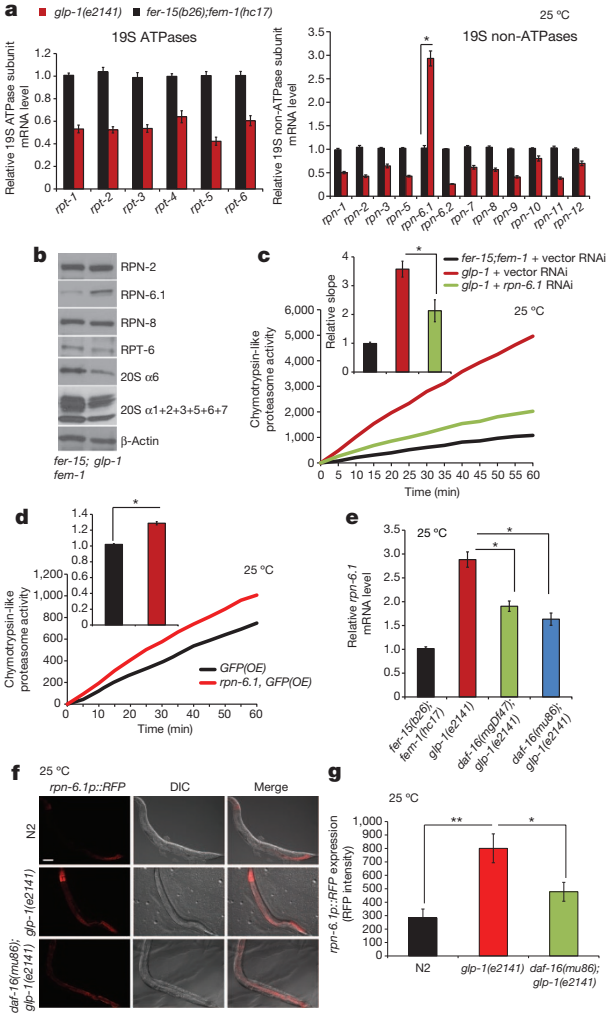

Figure 3 | DAF-16 is necessary for increased expression of *rpn-6.1* in *glp-1* mutants. **a**, Data represent the mean ± s.e.m. of the relative expression levels to *fer-15(b26);fem-1(hc17)* ($n = 11$, $P = 2.09 \times 10^{-6}$). **b**, Western blot analysis of RPN-2, RPN-6.1, RPN-8, RPT-6, α6 and α1+2+3+5+6+7. β-Actin is the loading control. **c**, *glp-1* mutants fed *rpn-6.1* RNAi bacteria starting day 1 of adulthood have decreased chymotrypsin-like proteasome activity ($P < 0.05$). Proteasome activity (relative slope to *fer-15(b26);fem-1(hc17)*) represents the mean ± s.e.m. ($n = 6$). **d**, Increased chymotrypsin-like proteasome activity in *rpn-6.1* overexpressing N2 worms (*rpn-6.1*, *GFP(OE)*) in day 1 adult worm extract ($P < 0.001$). Proteasome activity (relative slope to *GFP(OE)* worms) represents the mean ± s.e.m. ($n = 9$). **e**, *daf-16;glp-1* double mutants have decreased *rpn-6.1* mRNA levels ($P < 0.001$). Graph represents the mean ± s.e.m. ($n = 6$). **f**, Representative images of RFP expressed under control of the *rpn-6.1* promoter. *rpn-6.1* is expressed in the pharynx and posterior intestine in N2 worms. Increased *rpn-6.1* expression in *glp-1(e2141)* animals relative to N2. *daf-16;glp-1* mutant worms have decreased *rpn-6.1* expression compared to *glp-1* mutants. DIC, differential interference contrast microscopy. Scale bar, 100 μm. **g**, Quantification of RFP signal intensity (mean ± s.e.m. ($n = 5$)). *glp-1(e2141)* worms have increased *rpn-6.1* expression compared to N2 ($P < 0.01$) and *daf-16(mu86);glp-1(e2141)* double mutants ($P < 0.05$). All statistical comparisons were made by Student's *t*-test for unpaired samples.

daf-16;glp-1 double mutants, we found almost a twofold decreased expression of *rpn-6.1* compared to *glp-1(e2141)* worms, although *rpn-6.1* expression is still increased compared to wild-type worms (Fig. 3f, g). These results correlated with quantitative real-time polymerase chain reaction (qPCR) data indicating that *daf-16* mutations decrease *rpn-6.1* expression in *glp-1* mutants, but not to control levels (Fig. 3e, g), suggesting that a potential additional factor may be necessary for *rpn-6.1* expression in addition to DAF-16.

rpn-6.1 determines stress resistance

With the strong connection between *daf-16*, a key ageing modulator, *rpn-6.1*, a key proteasomal factor, and increased proteasome activity in long-lived *glp-1* mutant animals dependent upon both *daf-16* and *rpn-6.1*, we asked what role, if any, does *rpn-6.1* have in longevity. To assess the requirement for *rpn-6.1* during lifespan, we conducted RNAi knock down of this gene in *C. elegans*. Because proteasomal function is required during larval development[33], we initiated *rpn-6.1* RNAi treatment during adulthood, the time at which *daf-16* is required for longevity assurance[19]. Knock down of *rpn-6.1* substantially decreased the lifespan of *glp-1* mutant animals (Supplementary Fig. 19). However, loss of *rpn-6.1* also decreased lifespan of both wild-type and sterile control animals (*fer-15(b26);fem-1(hc17)*). In addition to germ-cell loss, we also examined the effects of *rpn-6.1* RNAi on other pathways that influence lifespan such as reduced IIS (*daf-2(e1370)* worms), reduced mitochondrial electron transport chain (*isp-1(qm150)* worms) and reduced food intake (*eat-2(ad1116)* worms). In all cases, knock down of *rpn-6.1* substantially decreased lifespan, confirming that this gene is essential for the viability of adult animals, making lifespan analysis by *rpn-6.1* loss of function difficult to interpret (Supplementary Fig. 19).

To explore whether *rpn-6.1* might have a positive role in longevity, we tested the impact of increased *rpn-6.1* expression. We overexpressed *rpn-6.1* in wild-type worms and conducted a series of physiological assays to measure the effects of *rpn-6.1* overexpression (OE) on resistance to challenges of oxidative stress, heat-shock and ultraviolet (UV) damage, all of which are correlated with increased longevity. *rpn-6.1(OE)* nematodes were significantly more resistant, than control strains, to oxidative stress induced by growing the worms in the presence of paraquat (Fig. 4a and Supplementary Fig. 20a). Under heat stress (34 °C), *rpn-6.1(OE)* worms lived markedly longer than control strains (Fig. 4b and Supplementary Fig. 20b). Interestingly, increased levels of *rpn-6.1* did not result in global upregulation of all stress responses because *rpn-6.1(OE)* did not protect against UV damage (Fig. 4c and Supplementary Fig. 20c). Because overexpression of *rpn-6.1* increased resistance to conditions that challenge the proteome, we examined whether it also resulted in lifespan extension. *rpn-6.1(OE)* did not extend the lifespan of worms at 20 °C but it did at 25 °C, a temperature that results in mild heat stress (Fig. 4d and Supplementary Fig. 20d). *daf-16* RNAi treatment blocked the lifespan extension induced by *rpn-6.1(OE)* at 25 °C (Fig. 4e and Supplementary Fig. 20e). Therefore, under conditions of proteome stress, overexpression of *rpn-6.1* is sufficient to promote increased survival. As a more formal test, we asked whether animals with a reduced heat-shock response via *hsf-1* downregulation had increased survival when *rpn-6.1* was overexpressed. *hsf-1*-RNAi-treated *rpn-6.1(OE)* worms were long-lived compared to control strains under the same treatment (Fig. 4f and Supplementary Fig. 20f). This last result not only indicates that the lifespan extension induced by *rpn-6.1(OE)* is *hsf-1* independent, but also suggests that these worms can significantly overcome the loss of this critical transcription factor required for adult lifespan, heat-shock and proteotoxicity responses.

Intrigued by the protection that *rpn-6.1* overexpression could confer, we hypothesized that RPN-6.1 could be a potential candidate to correct protein homeostasis deficiencies underlying diseases such as Alzheimer's, Parkinson's or Huntington's disease. Because the latter disease has been associated with proteasome failure[34], we tested whether increased levels of *rpn-6.1* could have beneficial effects in a polyglutamine (polyQ) disease model. Worm motility is markedly reduced by the aggregation of polyQ expression in neurons, with a pathogenic threshold at a length of 35–40 glutamines[35]. Notably, *rpn-6.1* overexpression substantially improved motility and reduced toxicity of worms expressing polyQ40 and polyQ67 (Fig. 5a and Supplementary Fig. 21). In addition, loss of *rpn-6.1* had a detrimental effect on the motility phenotype of polyQ67 worms even at early (day 3) adulthood stages (Fig. 5b and Supplementary Fig. 22). Furthermore,

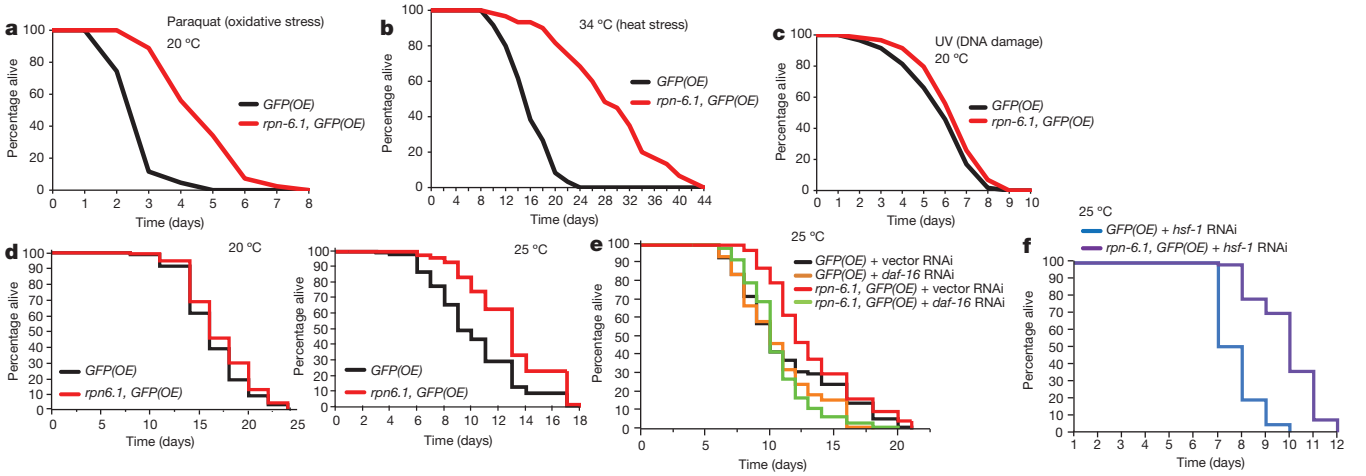

Figure 4 | *rpn-6.1* is a determinant of stress resistance and viability. **a**, *rpn-6.1* overexpressing (OE) worms live longer than controls under oxidative stress (log rank, $P < 0.0001$, *GFP(OE)*: mean = 2.97 ± 0.10, $n = 43/60$; *rpn-6.1, GFP(OE)*: mean = 4.89 ± 0.17, $n = 40/59$). **b**, *rpn-6.1(OE)* worms live longer than controls under heat stress conditions (34 °C) (log rank, $P < 0.0001$, *GFP(OE)*: mean = 16.20 ± 0.47, $n = 60/60$; *rpn-6.1, GFP(OE)*: mean = 29.83 ± 0.99, $n = 60/60$). **c**, Ultraviolet stress assay on *rpn-6.1(OE)* worms (log rank, $P = 0.06$, *GFP(OE)*: mean = 6.01 ± 0.27, $n = 59/60$; *rpn-6.1, GFP(OE)*: mean = 6.57 ± 0.19, $n = 58/59$). **d**, *rpn-6.1(OE)* does not affect lifespan at 20 °C (log rank, $P = 0.15$, *GFP(OE)*: mean = 16.33 ± 0.34, $n = 90/100$; *rpn-6.1, GFP(OE)*: mean = 17.05 ± 0.34, $n = 95/100$). *rpn-6.1* overexpression extends lifespan at 25 °C (log rank, $P < 0.0001$, *GFP(OE)*: mean = 10.19 ± 0.32, $n = 109/120$; *rpn-6.1, GFP(OE)*: mean = 12.73 ± 0.29, $n = 113/120$). **e**, *daf-16* RNAi (starting at day 1 of adulthood) blocks lifespan extension induced by *rpn-6.1* overexpression (*rpn-6.1, GFP(OE)* fed vector RNAi bacteria versus *rpn-6.1, GFP(OE)* fed *daf-16* RNAi bacteria, log rank, $P < 0.0001$). *GFP(OE)* fed vector RNAi bacteria: mean = 11.36 ± 0.45, $n = 86/100$; *GFP(OE)* fed *daf-16* RNAi bacteria: mean = 10.59 ± 0.36, $n = 77/100$; *rpn-6.1, GFP(OE)* fed vector RNAi bacteria: mean = 13.27 ± 0.37, $n = 87/100$; *rpn-6.1, GFP(OE)* fed *daf-16* RNAi bacteria: mean = 10.59 ± 0.28, $n = 88/100$. **f**, *hsf-1*-RNAi-treated *rpn-6.1(OE)* worms were long-lived compared to controls (log rank, $P < 0.0001$). RNAi was initiated at day 1 of adulthood. *GFP(OE)* fed *hsf-1* RNAi bacteria: mean = 7.74 ± 0.09, $n = 93/99$; *rpn-6.1, GFP(OE)* fed *hsf-1* RNAi bacteria: mean = 9.92 ± 0.13, $n = 94/100$. See Supplementary Table 5 for statistical analysis and replicate data of stress assays and lifespan experiments.

we observed by filter trap analysis that *rpn-6.1(OE)* reduced polyQ aggregate levels whereas polyQ67 total protein levels remained constant (Fig. 5c), suggesting that *rpn-6.1* specifically reduces aggregated, but not soluble, polyQ proteins.

Discussion

A growing body of evidence suggests that the protective modulation of various nodes of the proteostasis network, including the heat-shock response and autophagy, can contribute to the extended lifespan caused by the IIS[36,37], diet restriction[38] and germline-signalling pathways[39]. We report evidence for the requirement of an upregulated proteasome activity in the extended lifespan of germline-deficient nematodes. Our initial analysis of proteasome activity among different longevity models in the worm reveals that only *glp-1* mutant and diet-restricted animals share an increased proteasome activity, and we hypothesize that these animals may share a strategy in which resources are actively re-allocated from the germ line to the soma, resulting in an enhanced protection of the proteome within somatic cells. Furthermore, we find distinct differences in the proteasome activity between *glp-1* and *daf-2* mutant animals that is mediated by DAF-16, and in part by KRI-1, DAF-12 and DAF-9, confirming previous genetic suggestions that DAF-16 activity is differentially regulated between *glp-1* and *daf-2* mutants. Mechanistically, in germline-deficient animals, *rpn-6.1* and subsequent increases in proteasome activity seem to be direct downstream targets of DAF-16/FOXO. Our results thus provide new insights into proteostasis regulation and provide a link between the longevity regulator DAF-16 and proteasome activity regulation upon *rpn-6.1* expression.

We further define RPN-6 as a potent factor to increase resistance to proteotoxic stress, as its upregulation can delay the deleterious effects of strong adverse conditions. It is intriguing to speculate that one method to ensure survival of the soma may be the direct activation of FOXO/*daf-16*, under limited nutrient availability or loss of the germ line, resulting in increased *rpn-6.1* levels and increased proteome maintenance. Recently, it has been reported that changes in the proteasome may explain why ageing is a risk factor for neurodegenerative diseases such

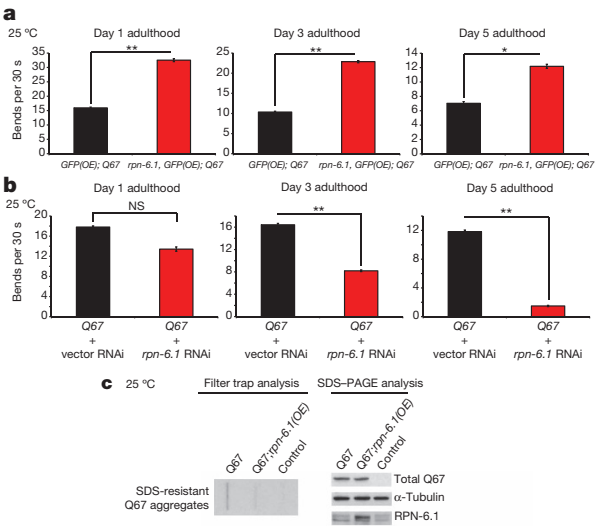

Figure 5 | *rpn-6.1* protects from polyglutamine aggregation. **a**, *rpn-6.1* improves motility in polyQ67 worms. Bar graphs represent average (±s.e.m.) thrashing over a 30-s period on day 1 ($P < 0.0001$, *GFP(OE);Q67* ($n = 40$), *rpn-6.1,GFP(OE);Q67* ($n = 41$)), day 3 ($P < 0.0001$, *GFP(OE);Q67* ($n = 40$), *rpn-6.1,GFP(OE);Q67* ($n = 44$)) and day 5 ($P < 0.05$, *GFP(OE);Q67* ($n = 31$), *rpn-6.1,GFP(OE);Q67* ($n = 39$)) of adulthood. **b**, Loss of *rpn-6.1* has a detrimental effect on the motility defects of polyQ67 worms. Bar graphs represent average (±s.e.m.) thrashing over a 30-s period on day 1 ($P = 0.15$, *Q67* fed vector RNAi bacteria ($n = 58$), *Q67* fed *rpn-6.1* RNAi bacteria ($n = 30$)), day 3 ($P < 0.0001$, *Q67* fed vector RNAi bacteria ($n = 44$), *Q67* fed *rpn-6.1* RNAi bacteria ($n = 51$)) and day 5 ($P < 0.0001$, *Q67* fed vector RNAi bacteria ($n = 41$), *Q67* fed *rpn-6.1* RNAi bacteria ($n = 47$)) of adulthood. All statistical comparisons were made by Student's *t*-test for unpaired samples. **c**, Filter trap analysis indicates that *rpn-6.1* overexpression results in reduced polyQ aggregates (detected by anti-GFP antibody). Right panel: SDS–PAGE analysis with antibodies to GFP, RPN-6 and α-tubulin loading control. *$P < 0.05$; **$P < 0.0001$.

as Alzheimer's, Parkinson's and Huntington's disease[40]. Therefore, RPN-6 may be a powerful candidate to correct deficiencies in disorders associated with a failure in protein homeostasis. It will be of crucial interest to explore in mammalian models whether RPN-6 could indeed alleviate the associated symptoms of these disorders.

METHODS SUMMARY

Caenorhabditis elegans were cultured using standard techniques[41] and fed on *Escherichia coli* OP50 or HT115 containing a double-stranded-RNA-expressing plasmid[42].

26S proteasome activity assays. *In vitro* 26S proteasome activity assays were performed as previously described[27]. Worms were lysed in proteasome activity assay buffer (50 mM Tris-HCl, pH 7.5, 250 mM sucrose, 5 mM $MgCl_2$, 0.5 mM EDTA, 2 mM ATP and 1 mM dithiothreitol) using a Precellys 24 homogenizer (Bertin technologies). Lysate was centrifuged at 10,000*g* for 15 min at 4 °C. A total of 25 μg of total protein lysate was transferred to a 96-well microtitre plate (BD Falcon) and incubated with fluorogenic substrate. Fluorescence (380-nm excitation, 460-nm emission) was monitored on a microplate fluorometer (Infinite M1000, Tecan) every 5 min for 1 h at 25 °C.

Motility assay. Thrashing rate was determined as previously described[35]. Worms were transferred to a drop of M9 buffer and after 30 s of adaptation the number of body bends was counted for 30 s. A body bend was defined as a change in direction of the bend at the midbody of a nematode[43].

Filter trap. Worm extracts were generated by glass bead disruption on ice in non-denaturing lysis buffer (50 mM HEPES, pH 7.4, 150 mM NaCl, 1 mM EDTA, 0.5% Triton X-100) supplemented with EDTA-free protease inhibitor cocktail (Roche). Lysate was centrifuged at 5,000*g* for 5 min. A total of 70 μg of protein extract was supplemented with SDS at a final concentration of 1% and loaded onto a cellulose acetate membrane assembled in a slot blot apparatus (BioRad). The membrane was washed with 0.1% SDS and retained Q67-GFP was assessed by immunoblotting for GFP (Roche).

A detailed description of all experimental methods including *C. elegans* strains, growth, imaging, lifespan analysis, stress assays and RNAi application is provided in Methods.

Full Methods and any associated references are available in the online version of the paper.

Received 8 August 2011; accepted 13 June 2012.
Published online 26 August 2012.

1. Kirkwood, T. B. Evolution of ageing. *Nature* **270,** 301–304 (1977).
2. Kenyon, C. A pathway that links reproductive status to lifespan in *Caenorhabditis elegans*. *Ann. NY Acad. Sci.* **1204,** 156–162 (2010).
3. Partridge, L., Gems, D. & Withers, D. J. Sex and death: what is the connection? *Cell* **120,** 461–472 (2005).
4. Shanley, D. P. & Kirkwood, T. B. Calorie restriction and aging: a life-history analysis. *Evolution* **54,** 740–750 (2000).
5. Arantes-Oliveira, N., Apfeld, J., Dillin, A. & Kenyon, C. Regulation of life-span by germ-line stem cells in *Caenorhabditis elegans*. *Science* **295,** 502–505 (2002).
6. Hsin, H. & Kenyon, C. Signals from the reproductive system regulate the lifespan of *C. elegans*. *Nature* **399,** 362–366 (1999).
7. Wang, M. C., O'Rourke, E. J. & Ruvkun, G. Fat metabolism links germline stem cells and longevity in *C. elegans*. *Science* **322,** 957–960 (2008).
8. Lin, K., Hsin, H., Libina, N. & Kenyon, C. Regulation of the *Caenorhabditis elegans* longevity protein DAF-16 by insulin/IGF-1 and germline signaling. *Nature Genet.* **28,** 139–145 (2001).
9. Berman, J. R. & Kenyon, C. Germ-cell loss extends *C. elegans* life span through regulation of DAF-16 by *kri-1* and lipophilic-hormone signaling. *Cell* **124,** 1055–1068 (2006).
10. Gerisch, B., Weitzel, C., Kober-Eisermann, C., Rottiers, V. & Antebi, A. A hormonal signaling pathway influencing *C. elegans* metabolism, reproductive development, and life span. *Dev. Cell* **1,** 841–851 (2001).
11. Bence, N. F., Sampat, R. M. & Kopito, R. R. Impairment of the ubiquitin-proteasome system by protein aggregation. *Science* **292,** 1552–1555 (2001).
12. Bennett, E. J., Bence, N. F., Jayakumar, R. & Kopito, R. R. Global impairment of the ubiquitin-proteasome system by nuclear or cytoplasmic protein aggregates precedes inclusion body formation. *Mol. Cell* **17,** 351–365 (2005).
13. Powers, E. T., Morimoto, R. I., Dillin, A., Kelly, J. W. & Balch, W. E. Biological and chemical approaches to diseases of proteostasis deficiency. *Annu. Rev. Biochem.* **78,** 959–991 (2009).
14. Lakowski, B. & Hekimi, S. The genetics of caloric restriction in *Caenorhabditis elegans*. *Proc. Natl Acad. Sci. USA* **95,** 13091–13096 (1998).
15. Dillin, A. *et al.* Rates of behavior and aging specified by mitochondrial function during development. *Science* **298,** 2398–2401 (2002).
16. Hamer, G., Matilainen, O. & Holmberg, C. I. A photoconvertible reporter of the ubiquitin-proteasome system *in vivo*. *Nature Methods* **7,** 473–478 (2010).
17. Mitchell, D. H., Stiles, J. W., Santelli, J. & Sanadi, D. R. Synchronous growth and aging of *Caenorhabditis elegans* in the presence of fluorodeoxyuridine. *J. Gerontol.* **34,** 28–36 (1979).
18. Priess, J. R., Schnabel, H. & Schnabel, R. The *glp-1* locus and cellular interactions in early *C. elegans* embryos. *Cell* **51,** 601–611 (1987).
19. Dillin, A., Crawford, D. K. & Kenyon, C. Timing requirements for insulin/IGF-1 signaling in *C. elegans*. *Science* **298,** 830–834 (2002).
20. Hansen, M., Hsu, A. L., Dillin, A. & Kenyon, C. New genes tied to endocrine, metabolic, and dietary regulation of lifespan from a *Caenorhabditis elegans* genomic RNAi screen. *PLoS Genet.* **1,** e17 (2005).
21. Cohen, E., Bieschke, J., Perciavalle, R. M., Kelly, J. W. & Dillin, A. Opposing activities protect against age-onset proteotoxicity. *Science* **313,** 1604–1610 (2006).
22. Hsu, A. L., Murphy, C. T. & Kenyon, C. Regulation of aging and age-related disease by DAF-16 and heat-shock factor. *Science* **300,** 1142–1145 (2003).
23. Alam, J. *et al.* Nrf2, a Cap'n'Collar transcription factor, regulates induction of the heme oxygenase-1 gene. *J. Biol. Chem.* **274,** 26071–26078 (1999).
24. An, J. H. & Blackwell, T. K. SKN-1 links *C. elegans* mesendodermal specification to a conserved oxidative stress response. *Genes Dev.* **17,** 1882–1893 (2003).
25. Goudeau, J. *et al.* Fatty acid desaturation links germ cell loss to longevity through NHR-80/HNF4 in *C. elegans*. *PLoS Biol.* **9,** e1000599 (2011).
26. Finley, D. Recognition and processing of ubiquitin-protein conjugates by the proteasome. *Annu. Rev. Biochem.* **78,** 477–513 (2009).
27. Kisselev, A. F. & Goldberg, A. L. Monitoring activity and inhibition of 26S proteasomes with fluorogenic peptide substrates. *Methods Enzymol.* **398,** 364–378 (2005).
28. Köhler, A. *et al.* The axial channel of the proteasome core particle is gated by the Rpt2 ATPase and controls both substrate entry and product release. *Mol. Cell* **7,** 1143–1152 (2001).
29. Pathare, G. R. *et al.* The proteasomal subunit Rpn6 is a molecular clamp holding the core and regulatory subcomplexes together. *Proc. Natl Acad. Sci. USA* **109,** 149–154 (2012).
30. Santamaria, P. G., Finley, D., Ballesta, J. P. & Remacha, M. Rpn6p, a proteasome subunit from *Saccharomyces cerevisiae*, is essential for the assembly and activity of the 26 S proteasome. *J. Biol. Chem.* **278,** 6687–6695 (2003).
31. Furuyama, T., Nakazawa, T., Nakano, I. & Mori, N. Identification of the differential distribution patterns of mRNAs and consensus binding sequences for mouse DAF-16 homologues. *Biochem. J.* **349,** 629–634 (2000).
32. Celniker, S. E. *et al.* Unlocking the secrets of the genome. *Nature* **459,** 927–930 (2009).
33. Ghazi, A., Henis-Korenblit, S. & Kenyon, C. Regulation of *Caenorhabditis elegans* lifespan by a proteasomal E3 ligase complex. *Proc. Natl Acad. Sci. USA* **104,** 5947–5952 (2007).
34. Li, X. J. &. L. i. S. Proteasomal dysfunction in aging and Huntington disease. *Neurobiol. Dis.* **43,** 4–8 (2011).
35. Brignull, H. R., Moore, F. E., Tang, S. J. & Morimoto, R. I. Polyglutamine proteins at the pathogenic threshold display neuron-specific aggregation in a pan-neuronal *Caenorhabditis elegans* model. *J. Neurosci.* **26,** 7597–7606 (2006).
36. Melendez, A. *et al.* Autophagy genes are essential for dauer development and life-span extension in *C. elegans*. *Science* **301,** 1387–1391 (2003).
37. Morley, J. F. & Morimoto, R. I. Regulation of longevity in *Caenorhabditis elegans* by heat shock factor and molecular chaperones. *Mol. Biol. Cell* **15,** 657–664 (2004).
38. Hansen, M. *et al.* A role for autophagy in the extension of lifespan by dietary restriction in *C. elegans*. *PLoS Genet.* **4,** e24 (2008).
39. Lapierre, L. R., Melendez, A. & Hansen, M. Autophagy links lipid metabolism to longevity in *C. elegans*. *Autophagy* **8,** 144–146 (2012).
40. Zabel, C. *et al.* Proteasome and oxidative phoshorylation changes may explain why aging is a risk factor for neurodegenerative disorders. *J. Proteomics* **73,** 2230–2238 (2010).
41. Brenner, S. The genetics of *Caenorhabditis elegans*. *Genetics* **77,** 71–94 (1974).
42. Fire, A. *et al.* Potent and specific genetic interference by double-stranded RNA in *Caenorhabditis elegans*. *Nature* **391,** 806–811 (1998).
43. Chai, Y., Shao, J., Miller, V. M., Williams, A. & Paulson, H. L. Live-cell imaging reveals divergent intracellular dynamics of polyglutamine disease proteins and supports a sequestration model of pathogenesis. *Proc. Natl Acad. Sci. USA* **99,** 9310–9315 (2002).

Supplementary Information is linked to the online version of the paper at www.nature.com/nature.

Acknowledgements We thank S. Panowski for help with the generation of transgenic strains. We thank D. Joyce for proteasome activity assays and S. Wolff for comments on the manuscript. This work was supported by HHMI and the NIA. D.V. was a recipient of the F.M. Kirby, Inc. Foundation Postdoctoral Scholar Award and Beatriu de Pinós (AGAUR) fellowship.

Author Contributions D.V. and A.D. planned and supervised the project. D.V. performed the experiments, data analysis and interpretation. I.M. performed biochemistry experiments and contributed to other assays. Z.L. performed UPS reporter experiment, lifespans and injections. P.M.D. performed the filter trap assay. C.M. performed immunoblots. A.P.C.R. and G.M. performed the transcription factor binding site analysis. The manuscript was written by D.V. and A.D. and edited by I.M. and C.M. All authors discussed the results and commented on the manuscript.

Author Information Reprints and permissions information is available at www.nature.com/reprints. The authors declare no competing financial interests. Readers are welcome to comment on the online version of this article at www.nature.com/nature. Correspondence and requests for materials should be addressed to A.D. (dillin@salk.edu).

METHODS

***Caenorhabditis elegans* strains and generation of transgenic lines.** CF512 (*fer-15(b26)II;fem-1(hc17)IV*), CB4037 (*glp-1(e2141)III*), AU147 (*daf-16(mgDf47)I;glp-1(e2141)III*), CF1880 (*daf-16(mu86)I;glp-1(e2141)III*), DA1116 (*eat-2(ad1116)II*) and wild-type (N2) *C. elegans* strains were obtained from the *Caenorhabditis* Genetic Center. AGD151 (*eat-2(ad1116)II; fer-15(b26)II;fem-1(hc17)IV*) was generated by crossing CF512 with DA1116 (*eat-2(ad1116)II*). CF596 (*daf-2(mu150)III*; *fer-15(b26)II;fem-1(hc17)IV*) was a gift from C. Kenyon. *C. elegans* were handled using standard methods[41].

For the generation of worm strains AGD597–AGD598 (N2, *uthEx556[psur5::rpn-6.1, pmyo3::GFP]* and N2, *uthEx556[psur5::rpn-6.1, pmyo3::GFP]*), a DNA plasmid mixture containing 75 ng μl^{-1} pDV1 (*psur5::rpn-6.1*) and 20 ng μl^{-1} pPD93_97 (*pmyo-3::GFP*) was injected into the gonads of adult N2 hermaphrodite animals, using standard methods[44]. GFP-positive F_1 progeny were selected. Individual F_2 worms were isolated to establish independent lines. Control worms (AGD614) used in experiments with AGD597–AGD598 were generated by microinjecting N2 worms with 20 ng μl^{-1} pPD93_97 (*pmyo-3::GFP*). AGD886 (*fer-15(b26)II; fem-1(hc17)IV; uthEx557[psur5::rpn-6.1, pmyo3::GFP])* was generated by crossing AGD598 to CF512. Control strain AGD885 (*fer-15(b26)II;fem-1(hc17)IV; uthEx633[myo3p::GFP]*) was generated by crossing AGD614 to CF512.

Both AM101 (*rmIs110[pF25B3.3::Q40::YFP]*) and AM716 (*rmIs284 [pF25B3.3::Q67::YFP]*) were a gift from R. I. Morimoto. For the generation of worm strains AGD850 (*rmIs110[pF25B3.3::Q40::YFP];uthEx557[psur5::rpn-6.1,pmyo3::GFP]*) and AGD851 (*rmIs284[pF25B3.3::Q67::YFP];uthEx557 [psur5p::rpn-6.1,pmyo3::GFP]*), AGD598 strain was crossed to AM101 and AM716, respectively. Control strains AGD866 (*rmIs110[pF25B3.3::Q40::YFP]; uthEx633[pmyo3::GFP*]) and AGD867 (*rmIs284[pF25B3.3::Q67::YFP];;uthEx633 [pmyo3::GFP]*) were generated by crossing AGD614 to AM101 and AM716, respectively.

For the generation of worm strains AGD945–AGD946 (N2, *uthEx649[rpn-6p::tdTomato, pRF4(rol-6)]* and N2, *uthEx650[rpn-6p::tdTomato, pRF4(rol-6)]*), a DNA plasmid mixture containing 75 ng μl^{-1} pDV2 (*rpn-6p::tdTomato*) and 20 ng μl^{-1} *pRF4(rol-6)* was injected into the gonads of adult N2 hermaphrodite animals. Roller-phenotype-positive F_1 progeny were selected. Individual F_2 worms were isolated to establish independent lines. AGD1047 (*glp-1(e2141)III; uthEx649[rpn-6p::tdTomato, pRF4(rol-6)*) was generated by crossing AGD945 to CB4037. AGD1048 (*daf-16(mu86)I;glp-1(e2141)III; uthEx649[rpn-6p::tdTomato, pRF4(rol-6)*) was generated by crossing AGD945 to CF1880.

YD1 (N2, *xzEx1[Punc-54::Dendra2]*) and YD3 (N2, *xzEx3[Punc-54::UbG76V::Dendra2]*) were a gift from C. I. Holmberg. AGD1032 (*glp-1(e2141)III; xzEx1[Punc-54::Dendra2]*) was generated by crossing YD1 to CB4037. AGD1033 (*glp-1(e2141)III; xzEx3[Punc-54::UbG76V::Dendra2]*) was generated by crossing YD3 to CB4037. AGD1036 (*fer-15(b26)II;fem-1(hc17)IV; xzEx1[Punc-54::Dendra2])* was generated by crossing YD1 to CF512. AGD1037 (*fer-15(b26)II;fem-1(hc17)IV; xzEx3[Punc-54::UbG76V::Dendra2]*) was generated by crossing YD3 to CF512.

Construction of *rpn-6.1* expression construct. To construct pDV1, the *rpn-6.1 C. elegans* expression plasmid pPD95.77 from the Fire Lab kit was digested with SphI and XmaI to insert 3.6 kilobases of the *sur5* promoter. The resultant vector was then digested with KpnI and EcoRI to excise GFP and insert a multi-cloning site containing KpnI, NheI, NotI, XbaI and EcoRI. F57B9.10.A (*rpn-6.1*) was PCR amplified from cDNA to include 5′ XmaI and 3′ XbaI restriction sites then cloned into the aforementioned vector. All constructs were sequence verified.

Construction of *rpn-6.1* transcriptional reporter construct. To construct pDV2, pPD95.77 from the Fire Lab kit was digested to replace GFP with tdTomato. The promoter region and first intron of F57B9.10.A (*rpn-6.1*) was PCR amplified from N2 gDNA to include −363 to +1012 then cloned into the aforementioned vector using SalI and BamHI. The construct includes 46 nucleotides of exon 1. Construct was sequence verified.

RNAi constructs. RNAi-treated strains were fed *E. coli* (HT115) containing an empty control vector (L4440) or expressing double-stranded RNAi[42]. *daf-12*, *rpn-2*, *rpn-6.1*, *rpn-11* and *skn-1* RNAi constructs used were taken from the Vidal RNAi library. *cco-1*, *rpn-1*, *nhr-80*, *daf-9*, *hsf-1* and *kri-1* RNAi constructs used were from the Ahringer RNAi library. pAD43, the *daf-16* RNAi construct, was previously described[19]. See Supplementary Table 6 for further details about double-stranded RNAi constructs used for knockdown assays.

Lifespan studies. Lifespan analyses were performed as described previously[19]. Worms were synchronized by egg laying during 2 h. Animals were grown at 20 °C until day 1 of adulthood. One-hundred animals were used per condition and scored every day or every other day. Lifespans were conducted at either 20 °C or 25 °C as stated in the figure legends. For non-integrated lines AGD597, AGD598 and AGD886, GFP-positive worms were selected for lifespan studies. JMP IN 8 software was used for statistical analysis to determine means and percentiles. In all cases, *P* values were calculated using the log-rank (Mantel–Cox) method. See Supplementary Table 5 for statistical analysis and replicate data.

Stress assays. For heat-shock assays, eggs were transferred to plates seeded with *E. coli* (OP50) bacteria and grown to day 1 of adulthood at 20 °C. Worms were then transferred to fresh plates and heat shocked at 34 °C. Worms were checked every hour for viability. Paraquat assays were performed as previously described[45]. Briefly day-1 adults were transferred to plates containing 7.5 mM paraquat and cultured at 25 °C. Worms were checked every day for viability. For UV irradiation assays[46], day-5 adult worms were transferred to plates without OP50 and exposed to 1,200 J m^{-1} of UV using a UV Stratalinker. Worms were transferred back to fresh plates seeded with *E. coli* (OP50) and scored daily for viability.

Motility assay. Thrashing rate was determined as previously described[35]. Animals were grown at 20 °C until L4 stage and then grown at 25 °C for the rest of the experiment. Worms were fed with *E. coli* (OP50) bacteria. RNAi-treated strains were fed *E. coli* (HT115) containing an empty control vector (L4440) or expressing double-stranded RNAi of the *rpn-6.1* gene. Worms were transferred at day 1, 3 or 5 of adulthood to a drop of M9 buffer and after 30 s of adaptation the number of body bends was counted for 30 s. A body bend was defined as change in direction of the bend at the midbody of an animal[43].

26S proteasome fluorogenic peptidase assays. *In vitro* 26S proteasome activity assays were performed as previously described[27]. Briefly, worms were lysed in proteasome activity assay buffer (50 mM Tris-HCl, pH 7.5, 250 mM sucrose, 5 mM $MgCl_2$, 0.5 mM EDTA, 2 mM ATP and 1 mM dithiothreitol) using a Precellys 24 homogenizer (Bertin technologies). Lysate was centrifuged at 10,000*g* for 15 min at 4 °C. For each experiment, 25 µg of total protein lysate was transferred to a 96-well microtitre plate (BD Falcon) then fluorogenic substrate was added. For measuring the chymotrypsin-like activity of the proteasome either Z-Gly-Gly-Leu-AMC (Enzo) or Suc-Leu-Leu-Val-Tyr-AMC (Enzo) was used. Z-Leu-Leu-Glu-AMC (Enzo) was used to measure the caspase-like activity of the proteasome and Ac-Arg-Leu-Arg-AMC for the proteasome trypsin-like activity. Fluorescence (380-nm excitation, 460-nm emission) was monitored on a microplate fluorometer (Infinite M1000, Tecan) every 5 min for 1 h at 25 °C.

Western blot. For each strain, 2,000 adult worms were collected in proteasome assay activity buffer supplemented with protease inhibitors (Roche) and lysed using a Precellys 24 homogenizer. Lysate was centrifuged at 10,000*g* for 15 min at 4 °C. 40 µg of total protein was resolved by SDS–PAGE and transferred to nitrocellulose membrane. Western blot analysis was performed with anti-20S alpha 1–7 (Abcam), anti-proteasome 20S C2 (Abcam), anti-Rpt6 (Enzo), anti-Rpt5 (Enzo), anti-PSMD7 (Abcam), anti-Rpn2 (Abcam), anti-PSMD11 (Novus), anti-FK1 (Enzo), GFP (Roche), anti-α-tubulin (Sigma) and anti-β-actin (Abcam).

Filter trap. Animals were grown at 20 °C until L4 stage and then grown at 25 °C for the rest of the experiment. Day 1 adult worms were collected with M9 buffer and worm pellets were frozen with liquid N2. Frozen worm pellets were thawed on ice and worm extracts were generated by glass bead disruption on ice in non-denaturing lysis buffer (50 mM HEPES, pH 7.4, 150 mM NaCl, 1 mM EDTA, 0.5% Triton X-100) supplemented with EDTA-free protease inhibitor cocktail (Roche). Worm and cellular debris were removed with 5,000*g* spin for 5 min. Approximately 70 µg of protein extract was supplemented with SDS at a final concentration of 1% and loaded onto a cellulose acetate membrane assembled in a slot blot apparatus (BioRad). The membrane was washed with 0.1% SDS and retained Q67-GFP was assessed by immunoblotting for GFP (Roche). Extracts were also analysed by SDS–PAGE to determine protein expression levels.

Microscopy, image analysis, equipment and settings. Newly hatched larvae were grown at 25 °C until day 3 of adulthood. These young adults were mounted at room temperature (20–23 °C) on a 10% agarose pad on glass slides with 1 µl of M9, covered with cover slip. For imaging, Zeiss Axiovert microscope and AxioCam with software AxioVision Rel. 4.7 was used. Images of whole worms were acquired with 10 × 0.45 numerical aperture (NA) plan-apochromat objectives. Photoconversion was carried out using a 405-nm filter and an EXFO X-Cite 120Q metal halide lamp with 100% output for 60 s. Worms were imaged before and after photoconversion, and then were recovered on feeding plates at 20 °C. After 24 h, photoconverted worms were imaged with the same setting. Fluorescence intensities were analysed with AxioVision Rel. 4.7.

RNA isolation and quantitative RT–PCR. Total RNA was isolated from synchronized populations of approximately 2,000 day-5 adults. Total RNA was extracted using TRIzol reagent (GIBCO). cDNA was generated using Quantitect Reverse Transcriptase kit (Qiagen). SybrGreen real-time qPCR experiments were performed with a 1:20 dilution of cDNA using an ABI Prism79000HT (Applied Biosystems) following the manufacturer's instructions.

Data were analysed with the comparative $2\Delta\Delta C_t$ method using the geometric mean of *cdc-42*, *pmp-3* and *Y45F10D.4* as endogenous control[47]. See Supplementary Table 7 for details about the primers used for this assay.

44. Mello, C. C., Kramer, J. M., Stinchcomb, D. & Ambros, V. Efficient gene transfer in C.elegans: extrachromosomal maintenance and integration of transforming sequences. *EMBO J.* **10,** 3959–3970 (1991).
45. Vazquez-Manrique, R. P. *et al.* Reduction of *Caenorhabditis elegans* frataxin increases sensitivity to oxidative stress, reduces lifespan, and causes lethality in a mitochondrial complex II mutant. *FASEB J.* **20,** 172–174 (2006).
46. Wolff, S. *et al.* SMK-1, an essential regulator of DAF-16-mediated longevity. *Cell* **124,** 1039–1053 (2006).
47. Hoogewijs, D., Houthoofd, K., Matthijssens, F., Vandesompele, J. & Vanfleteren, J. R. Selection and validation of a set of reliable reference genes for quantitative sod gene expression analysis in *C. elegans*. *BMC Mol. Biol.* **9,** 9 (2008).